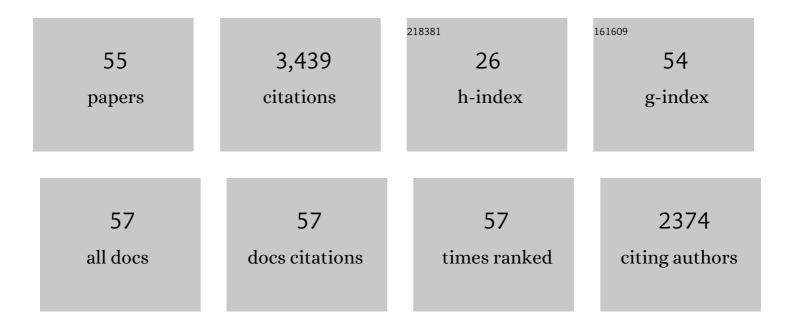
Jean Philippe Couzinié

List of Publications by Year in descending order

Source: https://exaly.com/author-pdf/1334466/publications.pdf Version: 2024-02-01



#	Article	IF	CITATIONS
1	Activation volume and the role of solute atoms in Al-Mg-Si alloy processed by equal channel angular extrusion. Journal of Alloys and Compounds, 2022, 899, 163334.	2.8	3
2	Experimental investigation of the local environment and lattice distortion in refractory medium entropy alloys. Scripta Materialia, 2022, 211, 114532.	2.6	1
3	Special Issue "Advanced Refractory Alloys― Metals, MDPI. Metals, 2022, 12, 333.	1.0	5
4	Cyclic hardening/softening and deformation mechanisms of a twip steel under reversed loading. Materialia, 2022, 22, 101421.	1.3	4
5	High-temperature deformation mechanisms in a BCC+B2 refractory complex concentrated alloy. Acta Materialia, 2022, 233, 117995.	3.8	21
6	High temperature phase stability of the compositionally complex alloy AlMo0.5NbTa0.5TiZr. Applied Physics Letters, 2021, 119, .	1.5	14
7	On the Room-Temperature Mechanical Properties of an Ion-Irradiated TiZrNbHfTa Refractory High Entropy Alloy. Jom, 2020, 72, 130-138.	0.9	34
8	Phase stability and microstructure evolution in a ductile refractory high entropy alloy Al10Nb15Ta5Ti30Zr40. Materialia, 2020, 9, 100569.	1.3	61
9	Ultrafine-Grained Two-Phase High-Entropy Alloy Microstructures Obtained via Recrystallization: Mechanical Properties. Frontiers in Materials, 2020, 7, .	1.2	4
10	Temperature dependent deformation behavior and strengthening mechanisms in a low density refractory high entropy alloy Al10Nb15Ta5Ti30Zr40. Materialia, 2020, 9, 100627.	1.3	47
11	Study of the stability under in vitro physiological conditions of surface silanized equimolar HfNbTaTiZr high-entropy alloy: A first step toward bio-implant applications. Surface and Coatings Technology, 2020, 385, 125374.	2.2	18
12	Effect of Mo, Ta, V and Zr on a duplex bcc+orthorhombic refractory complex concentrated alloy using diffusion couples. Intermetallics, 2020, 124, 106836.	1.8	2
13	Study of the FCC+L12 two-phase region in complex concentrated alloys based on the Al–Co–Cr–Fe–Ni–Ti system. Materialia, 2020, 14, 100905.	1.3	32
14	Body-centered cubic high-entropy alloys: From processing to underlying deformation mechanisms. Materials Characterization, 2019, 147, 533-544.	1.9	68
15	Temperature dependence of elastic moduli in a refractory HfNbTaTiZr high-entropy alloy. Journal of Alloys and Compounds, 2019, 799, 538-545.	2.8	42
16	Analysis of the fatigue crack growth mechanisms in equimolar body centered cubic HfNbTaTiZr high-entropy alloy: Discussions on its singularities and consequences on the crack propagation rate properties. Intermetallics, 2019, 110, 106459.	1.8	13
17	Ultrafine versus coarse grained Al 5083 alloys: From low-cycle to very-high-cycle fatigue. International Journal of Fatigue, 2019, 121, 84-97.	2.8	28
18	Hydrogen sorption in TiZrNbHfTa high entropy alloy. Journal of Alloys and Compounds, 2019, 775, 667-674	2.8	145

Jean Philippe Couzinié

#	Article	IF	CITATIONS
19	Study of a bcc multi-principal element alloy: Tensile and simple shear properties and underlying deformation mechanisms. Acta Materialia, 2018, 142, 131-141.	3.8	138
20	Thermodynamic instability of a nanocrystalline, single-phase TiZrNbHfTa alloy and its impact on the mechanical properties. Acta Materialia, 2018, 142, 201-212.	3.8	196
21	Comprehensive data compilation on the mechanical properties of refractory high-entropy alloys. Data in Brief, 2018, 21, 1622-1641.	0.5	105
22	Four-point bending fatigue behavior of an equimolar BCC HfNbTaTiZr high-entropy alloy: Macroscopic and microscopic viewpoints. Materialia, 2018, 4, 348-360.	1.3	26
23	From high-entropy alloys to complex concentrated alloys. Comptes Rendus Physique, 2018, 19, 721-736.	0.3	154
24	Development and exploration of refractory high entropy alloys—A review. Journal of Materials Research, 2018, 33, 3092-3128.	1.2	854
25	Synthesis of nanometric MoNbW alloy using self-propagating high-temperature synthesis. Advanced Powder Technology, 2017, 28, 1739-1744.	2.0	12
26	In situ TEM observations of dislocation dynamics in α titanium: Effect of the oxygen content. Materials Science & Engineering A: Structural Materials: Properties, Microstructure and Processing, 2017, 703, 331-339.	2.6	50
27	Design and tensile properties of a bcc Ti-rich high-entropy alloy with transformation-induced plasticity. Materials Research Letters, 2017, 5, 110-116.	4.1	153
28	Synthesis of nanometric refractory alloys powders in the Mo Nb W system. Journal of Alloys and Compounds, 2016, 679, 80-87.	2.8	8
29	Elastic and plastic properties of as-cast equimolar TiHfZrTaNb high-entropy alloy. Materials Science & Engineering A: Structural Materials: Properties, Microstructure and Processing, 2016, 654, 30-38.	2.6	146
30	Mechanical behavior and microstructure of Ti20Hf20Zr20Ta20Nb20 high-entropy alloy loaded under quasi-static and dynamic compression conditions. Materials Characterization, 2016, 111, 106-113.	1.9	82
31	On the room temperature deformation mechanisms of a TiZrHfNbTa refractory high-entropy alloy. Materials Science & Engineering A: Structural Materials: Properties, Microstructure and Processing, 2015, 645, 255-263.	2.6	189
32	Orientation imaging- ASTAR investigation of the grain and precipitate morphology in Al–Cu–Mg alloy processed by Equal Channel Angular Pressing. Journal of Alloys and Compounds, 2015, 647, 152-158.	2.8	6
33	In situ monitoring of the deformation mechanisms in titanium with different oxygen contents. Materials Science & Engineering A: Structural Materials: Properties, Microstructure and Processing, 2015, 636, 91-102.	2.6	106
34	Microstructural investigation of plastically deformed Ti20Zr20Hf20Nb20Ta20 high entropy alloy by X-ray diffraction and transmission electron microscopy. Materials Characterization, 2015, 108, 1-7.	1.9	84
35	Room-temperature creep and stress relaxation in commercial purity titanium–Influence of the oxygen and hydrogen contents on incubation phenomena and aging-induced rejuvenation of the creep potential. Materials Science & Engineering A: Structural Materials: Properties, Microstructure and Processing, 2015, 624, 79-89.	2.6	24
36	Microstructure of a near-equimolar refractory high-entropy alloy. Materials Letters, 2014, 126, 285-287.	1.3	135

#	Article	IF	CITATIONS
37	New structure in refractory high-entropy alloys. Materials Letters, 2014, 132, 123-125.	1.3	95
38	Surface-dependent oxidation of H 2 on CeO 2 surfaces. Journal of Catalysis, 2013, 297, 193-201.	3.1	109
39	Modeling of the influence of coarsening on viscoplastic behavior of a 319 foundry aluminum alloy. Materials Science & Engineering A: Structural Materials: Properties, Microstructure and Processing, 2013, 559, 40-48.	2.6	14
40	TEM and stress relaxation analysis of 99.1% aluminum processed by Equal Channel Angular Extrusion. IOP Conference Series: Materials Science and Engineering, 2012, 28, 012026.	0.3	0
41	Precipitation behaviour of Al3Zr precipitate in Al–Cu–Zr and Al–Cu–Zr–Ti–V alloys. Transactions of Nonferrous Metals Society of China, 2012, 22, 1860-1865.	1.7	42
42	Microstructural evolution of a recycled aluminum alloy deformed by equal channel angular pressing process. International Journal of Minerals, Metallurgy and Materials, 2012, 19, 1016-1022.	2.4	4
43	Microstructure investigation and thermal stability of 99.1% aluminum processed by equal channel angular extrusion. Journal of Materials Science, 2011, 46, 2185-2193.	1.7	4
44	Interaction Between Dislocations and Grain Boundaries Role in Plastic Deformation. Advanced Engineering Materials, 2010, 12, 1037-1040.	1.6	8
45	TEM and DSC Investigation of the Recovery of a Recycled Aluminum Processed by Equal Channel Angular Extrusion. Materials Science Forum, 2010, 667-669, 451-456.	0.3	1
46	Interactions between dislocations and interfaces – consequences for metal and ceramic plasticity. International Journal of Materials Research, 2010, 101, 1202-1210.	0.1	4
47	Characterization of aluminum processed by equal channel angular extrusion: Effect of processing route. Materials Characterization, 2009, 60, 1489-1495.	1.9	29
48	On the atomic structure of an asymmetrical near Σ = 27 grain boundary in copper. Philosophical Magazine Letters, 2009, 89, 757-767.	0.5	5
49	Atomic structures of symmetrical and asymmetrical facets in a near Σ=9{221} tilt grain boundary in copper. Acta Materialia, 2007, 55, 1791-1800.	3.8	25
50	Extended interfacial structure between two asymmetrical facets of a Σ = 9 grain boundary in copper. International Journal of Materials Research, 2006, 97, 954-957.	0.1	1
51	Interaction of dissociated lattice dislocations with a Σ=3 grain boundary in copper. International Journal of Plasticity, 2005, 21, 759-775.	4.1	43
52	In-situ transmission electron microscopy study of glissile grain boundary dislocation relaxation in a near Σ=3{111} grain boundary in copper. Materials Science & Engineering A: Structural Materials: Properties, Microstructure and Processing, 2005, 400-401, 264-267.	2.6	12
53	On the first steps of grain boundary dislocation stress relaxations in copper. International Journal of Materials Research, 2004, 95, 223-225.	0.8	4
54	On the interactions between dislocations and a near-Σ=3 grain boundary in a low stacking-fault energy metal. Philosophical Magazine Letters, 2003, 83, 721-731.	0.5	23

#	Article	IF	CITATIONS
55	High Strength and Electrical Conductivity of UFG Copper Alloys. Materials Science Forum, 0, 667-669, 755-759.	0.3	5